ELSEVIER

Advances in Colloid and Interface Science 123–126 (2006) 213–229

ADVANCES IN COLLOID AND INTERFACE SCIENCE

www.elsevier.com/locate/cis

Advances in adsorption of surfactants and their mixtures at solid/solution interfaces

Rui Zhang, P. Somasundaran *

Columbia University, NSF I/UCR Center for Novel Surfactants, 500 W 120th Street, New York, NY 10027, USA

Available online 17 October 2006

Abstract

Surfactants and their mixtures can drastically change the interfacial properties and hence are used in many industrial processes such as dispersion/flocculation, flotation, emulsification, corrosion inhibition, cosmetics, drug delivery, chemical mechanical polishing, enhanced oil recovery, and nanolithography. A review of studies on adsorption of single surfactant as well as mixtures of various types (anionic–cationic, anionic–nonionic, cationic–nonionic, cationic–zwitterionic and nonionic–nonionic) is presented here along with mechanisms involved. Results obtained using techniques such as zeta potential, flotation, AFM, specular neutron reflectivity, small angle neutron scattering, fluorescence, ESR, Raman spectroscopy, ellipsometry, HPLC and ATR-IR are reviewed along with those from traditional techniques to elucidate the mechanisms of adsorption and particularly to understand synergistic/antagonistic interactions at solution/liquid interfaces and nanostructures of surface aggregates. In addition, adsorption of several mixed surfactant systems is considered due to their industrial relevance. Finally an attempt is made to derive structure–property relationships to provide a solid foundation for the design and use of surfactant formulations for industrial applications.

Keywords: Adsorption; Surfactant; Mixtures; Aggregate structure; Adsorption model

Contents

* Corresponding author. Tel.: +1 212 854 2926; fax: +1 212 854 8362.
E-mail address: ps24@columbia.edu (P. Somasundaran).

0001-8686/$ - see front matter © 2006 Elsevier B.V. All rights reserved.
doi:10.1016/j.cis.2006.07.004

1. Introduction

Adsorption of surfactants on solid surfaces can modify their hydrophobicity, surface charge, and other key properties that govern interfacial processes such as flocculation/dispersion, flotation, wetting and adsolubilization, detergency, enhanced oil recovery, and corrosion inhibition [1–4].

In general, adsorption is governed by a number of forces such as covalent bonding, electrostatic attraction, hydrogen bonding or non-polar interactions between the adsorbed species, lateral associative interaction, solvation, and desolvation [5]. The total adsorption is usually the cumulative result of some or all of the above forces [6]. Mechanisms of surfactant adsorption are reviewed here in terms of various forces involved and factors controlling them. Importantly, adsorption of *mixed* surfactants is emphasized due to its relevance to practical systems that invariably use mixtures of several surfactants. Finally, models for adsorption of surfactants are examined for their validity for mixtures.

2. Mechanisms of surfactant adsorption

2.1. Standard free energy of adsorption

Adsorption can be considered as a partitioning of the adsorbate species between the interface and the bulk, and can occur if the interface is energetically favored by the surfactant in comparison to the bulk solution. Γ_δ, the adsorption density in the Stern plane δ, can be written as [6]:

$$\Gamma_\delta = lC\exp\left(\frac{-\Delta\overline{G^0_{ads}}}{RT}\right) \tag{1}$$

l is the effective length of the chain, C is the bulk concentration of the surfactant, R is the gas constant, T is the absolute temperature and $-\Delta\overline{G^0_{ads}}$ is the standard free energy of adsorption [6]. The driving force for adsorption is the sum of a number of contributing forces as mentioned above and $-\Delta\overline{G^0_{ads}}$ can be written as [5]:

$$\Delta\overline{G^0_{ads}} = \Delta G^0_{\text{elec}} + \Delta G^0_{\text{chem}} + \Delta G^0_{\text{c-c}} + \Delta G^0_{\text{c-s}} + \Delta G^0_{\text{H}} + \Delta G^0_{\text{H}_2\text{O}} + \ldots \tag{2}$$

where ΔG^0_{elec} is the electrostatic interaction term, ΔG^0_{chem} the chemical term due to covalent bonding, $\Delta G^0_{\text{c-c}}$ the free energy gained upon association of methyl groups in the hydrocarbon chain, $\Delta G^0_{\text{c-s}}$ the free energy due to interactions between the hydrocarbon chains and hydrophobic sites on the solid, ΔG^0_{H} the hydrogen bonding term and $\Delta G^0_{\text{H}_2\text{O}}$ is the term owing to dissolution or solvation of the adsorbate species or any species displaced from the interface due to adsorption. In the following section, the major forces involved in surfactant adsorption are discussed.

2.2. Driving forces for surfactant adsorption

For each surfactant–solid system, several of the above terms can be operative depending on the solid and the surfactant type, surfactant concentration, electrolyte, pH, temperature, etc.

2.2.1. Electrostatic interactions (ΔG^0_{elec})

In systems where the ionic surfactants and the solid particles are charged, electrostatic interactions play a governing role in the adsorption process.

$$\Delta G_{\text{elec}} = -zF\psi_\delta \tag{3}$$

where z is the valency of the adsorbate species, F the Faraday constant and Ψ_δ the potential in the δ.

Charge on the particle surface could be due to either the result of the hydrolysis of surface species in the case of oxides or due to the preferential dissolution of the lattice ions and subsequent adsorption of the resulting complexes. Role of electrostatic forces is clearly shown in Fig. 1, where the anionic surfactant sodium dodecyl sulfate [7,8] and cationic surfactant dodecylamine are shown to adsorb only on the positively charged calcite, resulting in flotation.

2.2.2. Chemical interactions (ΔG^0_{chem})

Chemical interaction is another important driving force for adsorption of surfactants on the solid particles. Compared to other driving forces, this interaction is specific to certain systems where covalent bonding can occur between the surfactant and the solid. For example, based on infrared studies, adsorption of fatty acids on fluorite and hematite has been attributed to

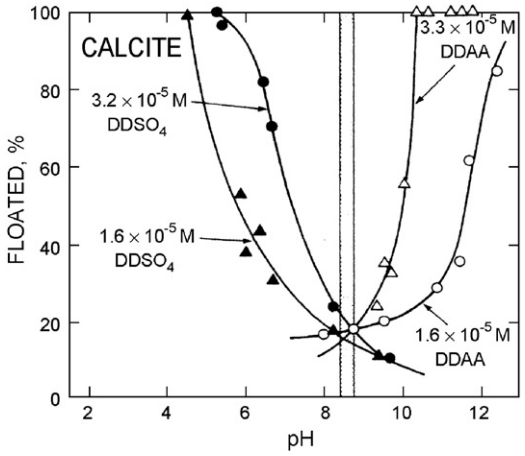

Fig. 1. Flotation of calcite using sodium dodecyl sulfate $DDSO_4$ and dodecylamine DDAA as a function of pH [9].

chemical bonding between the surfactant and the mineral surface [9,10,12]. In many cases, when the solubility limit is reached at the interface, precipitation of the surfactant can take place, leading in effect to multilayer adsorption. Thus, the sharp increase in the adsorption in Fig. 2 has been attributed to chemisorption caused by surface precipitation of hydrolyzed calcium ions.

2.2.3. Hydrophobic lateral interactions (ΔG^0_{c-c})

At concentrations above a threshold value, analogous to aggregation in the bulk, surfactant molecules tend to form two-dimensional aggregates at the solid/liquid interface, causing an abrupt increase in the adsorption density. These aggregates have been called as "hemi-micelles" [13] or, in general, "solloids" for surface colloids [14].

The hemi-micelle concept has been examined with the help of the flotation data shown in Fig. 3 [15] for a homologous series of alkylammonium acetates on negatively charged quartz. The sharp change in the flotation is the result of an increase in adsorption due to hydrophobic interactions upon hemi-micelle formation, which, in turn, depends on the chain lengths of the surfactants.

The driving force for adsorption (ΔG^0_{c-c}) results from the free energy of transferring the hydrocarbon chains from the aqueous environment into the hydrophobic interior of the aggregates. ΔG^0_{c-c} can be represented as a linear function of the energy (ϕ) gained per $-CH_2$ group [15].

$$\Delta G_{hyd} = -\frac{n(CH_2)\phi}{RT} \quad (4)$$

where $n(CH_2)$ is the number of CH_2 groups in the hydrocarbon chain.

ϕ, the energy for transfer of each $-CH_2$ has been estimated to be 1.0 kT, which is lower than that of transferring $-CH_2$ groups to saturated hydrocarbon phase but higher than that for transferring to a spherical micelle [16]. Evidently hemi-micelle is more tightly packed than micelles, with the hemi-micelles forming at concentrations below the corresponding critical micellar concentrations.

2.2.4. Hydrophobic interaction between the hydrocarbon chains and hydrophobic sites on the solid (ΔG^0_{c-s})

The hydrophobic interaction (ΔG^0_{c-s}) between the alkyl chain of a surfactant and the hydrophobic sites on the solid becomes a significant factor for surfactant adsorption on fully or partially hydrophobic surfaces. In this case, the surfactant molecules attach to the hydrophobic sites with the hydrocarbon chains aligning parallel to the surface at low concentrations and normal to the surface at higher concentrations. Such an adsorption process often results in a two-step isotherm.

2.2.5. Hydrogen bonding (ΔG^0_H)

Hydrogen bonding between surfactant species and the solid surface species could occur in systems containing hydroxyl, phenolic, carboxylic and amine groups on the surfactant. For instance, adsorption of a nonionic surfactant such as ethoxylated alcohol and sugar-based alkyl glucoside on oxides has been proposed to involve hydrogen bonding [17,18]. It should be noted that for adsorption due to hydrogen bonding to take place, the bond formed between the surfactant functional groups and mineral surfaces should be stronger than that formed between the mineral and interfacial water molecules.

2.2.6. Desolvation energy ($\Delta G^0_{H_2O}$)

When a hydrated head group of the surfactant transfers from the bulk to the mineral–solution interfacial region, partial removal of water from the secondary solvation shell around the surfactant head groups can occur. In contrast to other driving forces, desolvation energy due to such a process is unfavorable for adsorption process.

3. Adsorption of single surfactants

3.1. Adsorption isotherm

Adsorption isotherm [19–21] is commonly obtained by determining "depletion of the surfactant due to adsorption. From the saturation adsorption density at the solid/solution interface

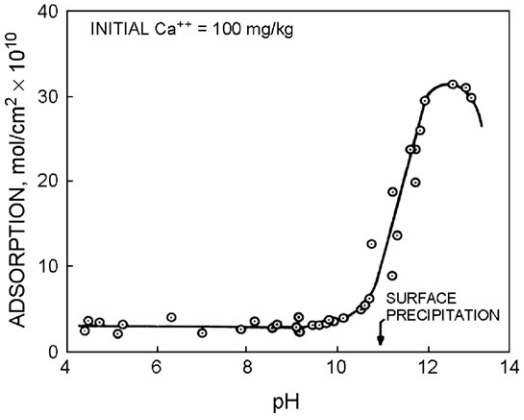

Fig. 2. pH dependence of calcium adsorption on quartz [11].

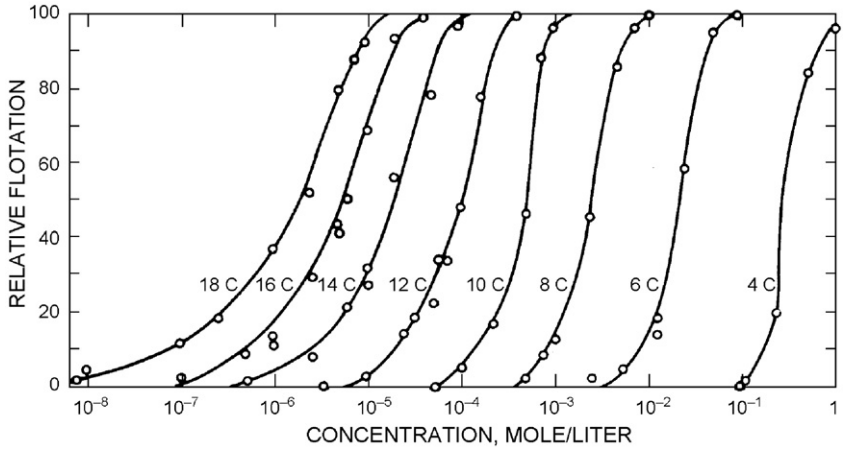

Fig. 3. The effect of alkyl chain length on the relative flotation response of quartz using alkylammonium acetate at pH 6–7 [14].

($\Gamma_{max,solid}$) and that at the air/solution interface ($\Gamma_{max,air}$), one can obtain an estimate of the number of layers, n_l, on the solid:

$$n_l = \frac{\Gamma_{max,solid}}{\Gamma_{max,air}} \quad (5)$$

Importantly, the surface coverage can provide information on the orientation of surfactant molecules in the adsorbed layer with the bilayers yielding a hydrophilic surface due to the polar or ionic heads of the surfactant oriented towards the bulk solution.

3.2. Adsorption isotherm of ionic surfactants

For adsorption of ionic surfactants on oppositely charged surface, the adsorption isotherm called "Somasundaran–Fuerstenau" isotherm, plotted on a log–log scale, is typically characterized by four regions [22]. The main features of this type of adsorption isotherm are illustrated in Fig. 4 for the adsorption of sodium dodecyl sulfate on alumina [23]:

Region 1. At low surfactant concentrations, the adsorption is due to electrostatic interaction between individual isolated charged monomeric species and the oppositely charged solid surface and the adsorption density follows the Gouy–Chapman equation with a slope of unity under constant ionic strength conditions.

Region 2. At the onset of region II, surfactant species begin to form surface aggregates, solloids (surface colloids), including hemi-micelles, admicelles, etc., due to lateral interactions between hydrocarbon chains. Due to this additional driving force resulting from the lateral association with the electrostatic interaction still active, the adsorption density exhibits a sharp increase in this stage.

Region 3. When the solid surface is electrically neutralized by the adsorbed surfactant ions, the electrostatic attraction is no longer operative and adsorption takes place due to lateral attraction alone with a reduced slope.

Region 4. When the surfactant concentration reaches critical micelle concentration, the surfactant monomer activity becomes constant and any further increase in concentration contributes only to the micellization in solution and it does not change the adsorption density. The adsorption in this region is mainly through lateral hydrophobic interaction between the hydrocarbon chains. In regions III and IV, surfactant molecules adsorb with a reversed orientation (head groups facing the bulk solution) resulting in a decrease in the hydrophobicity of the particles in this region.

Sometimes region III is not clearly identified in the case of adsorption of cationic surfactants on negatively charged surface due to loose packing of the cationic surface aggregates [24]. Also, a maximum is observed sometimes around region IV due to the presence of impurities [25], change in surfactant monomer concentration [26,27], or micellar exclusion [28] or precipitation [29].

Adsorption of ionic surfactants is usually reversible although hysteresis is observed in some cases. For example, adsorption of dodecylbenzenesulfonate on kaolin shows a positive hysteresis [30]. As mentioned in Section 2.2.1, pH plays a very significant role in controlling adsorption of ionic surfactants. Thus the

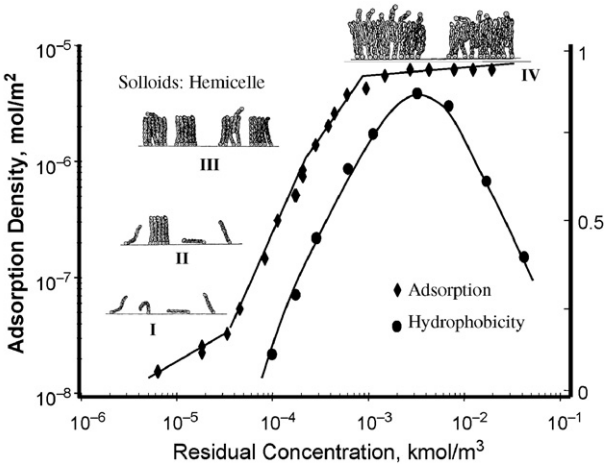

Fig. 4. The adsorption isotherm, hydrophobicity of sodium dodecyl sulfate on alumina at pH 6.5. The attached illustrations show the growth of surface aggregates and orientation of surfactant molecules [22].

Table 1
List of adsorption systems for ionic surfactants

Surfactant	Type	Solid	Technique	Reference
Sodium dodecyl sulfate	Anionic	Alumina	Adsorption, electrophoresis	[22]
Sodium dodecylbenzene sulfonate	Anionic	Kaolin	Abstraction, deabstraction	[35]
Xylenesulfonate (meta and para)	Anionic	Alumina, kaolin, anatase	Adsorption, microcalorimetry, electrokinetics, fluorescence	[31]
Sodium oleate	Anionic	Calcite	Flotation, SEM, microscope, electrokinetics, turbidity	[36]
4-*n*-Decylbenzenesulfonate (DBS)	Anionic	Kaolin, alumina	NMR, HPLC, adsorption, abstraction	[32]
4-*n*-Octylbenzenesulfonate	Anionic	Kaolin, alumina	NMR, HPLC, adsorption, abstraction	[32]
Ethoxylated sulfonate	Anionic	Kaolin, alumina	NMR, HPLC, adsorption, abstraction	[32]
Sodium oleate	Anionic	Hematite	Adsorption, calorimetry, abstraction, precipitation	[37]
Decylbenzenesulfonate	Anionic	Kaolin, alumina	Adsorption, abstraction	[34]
Sodium dodecyl sulfate	Anionic	Alumina	ESR	[38]
Sodium dodecyl sulfate	Anionic	Alumina	Raman	[39]
Potassium oleate	Anionic	Hematite	Flotation, surface tension	[40]
Na-dodecylbenzenesurfonate	Anionic	Kaolin	Adsorption, abstraction, solubility, precipitation	[29]
n-Decylbenzene sulfonate	Anionic	Alumina	Adsorption	[33]
n-Decylbenzene sulfonate	Anionic	Kaolin	Adsorption, desorption, HPLC, surface tension	[30]
Alkyl pyridinium salts	Anionic	Rutile	Adsorption	[23]
Alkyl benzene sulfonate	Anionic	Rutile	Adsorption	[23]
Tetradecyltrimethylammonium bromide	Cationic	Alumina	Electronic spin resonance, fluorescence, flotation	[24]
Dodecyltrimethylammonium bromide	Cationic	Alumina	Electronic spin resonance, fluorescence, flotation	[24]
Alkyltrimethylammonium bromide, C10-C16	Cationic	Silica sphere	Small angle neutron scattering	[41]
Dodecyl amine	Cationic	Hematite	Flotation	[42]
Tetradecyltrimethylammonium chloride	Cationic	Alumina	Adsorption, desorption, electrokinetics, fluroescence	[43]
Benzyldimethyldodecylammonium ions	Cationic	Silica	Adsorption, calorimetry, electrophoresis	[44]

adsorption of anionic surfactants is higher on positively charged surfaces (pH below isoelectric point (IEP)) than on negatively charged surfaces while the cationic surfactants adsorb more on negatively charged surfaces [22,24]. Molecular structure of surfactant does influence its adsorption behavior markedly. For example, while adsorption isotherms of 3,5-paraxylene and 2,5-paraxylene sulfonates [31] on alumina are similar, the adsorption of 2,4-metaxylene sulfonate is much lower than those of the other two. Calorimetric study of this system has shown that the adsorption is enthalpically driven at low surfactant concentrations while it is entropic at high concentrations. The entropy term for paraxylene sulfonates is higher than that for metasulfonate, suggesting compact packing of paraxylene sulfonate species in the surface aggregate. Insertion of ethoxylated group in the alkyl sulfonate chain has been found to enhance its adsorption in the premicellar region but decreases it in the micellar region [32]. The effect of hydrocarbons as additives on the adsorption of *n*-decylbenzene sulfonate on alumina has been shown to increase the sulfonate adsorption [33], especially in the low solution concentration range ($c < 10^{-4}$ M). In the case of alcohol, while propanol decreases the sulfonate adsorption, medium and long chain alcohols interact synergistically with the surfactant to enhance its adsorption. Surfactant adsorption is affected drastically also by the presence of soluble minerals due to interactions of dissolved mineral species with surfactant in the bulk leading to its precipitation [34]. There has been considerable work on the adsorption of ionic surfactants and the literature on this is given in Table 1 [35,36,40,42,43].

3.3. Adsorption of nonionic surfactants

Adsorption of nonionic surfactants is normally reversible with little hysteresis. Most nonionic surfactants contain polar groups that form hydrogen bonds with the hydroxyl groups on the solid surface. Since the hydrogen bonding is weaker than the electrostatic interaction, the adsorption of the nonionic surfactant to most solids is less than that of ionic surfactant. Nonionic surfactants exhibit adsorption isotherms similar to those of cationic surfactants, except for a sharp increase in region III of the adsorption isotherm because of the absence of electrostatic interactions. The adsorption of nonionic polyoxyethylene glycol surfactant on silica is presented in Fig. 5. In this case, the surface aggregates form mainly through hydrogen bonding interactions at low surfactant concentrations and through lateral associative interactions at high concentrations [44].

Polyoxyethylene glycol (EO) surfactants are by far the most studied surfactants due to their wide industrial applications [45–47]. Both EO and phenol EO surfactants behave similarly on silica surface in terms of their responses to parameters such as

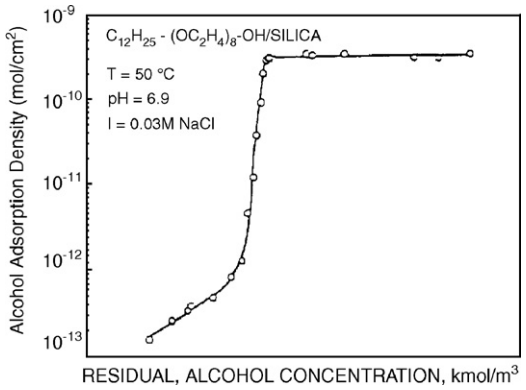

Fig. 5. Adsorption isotherm of dodecyloxyheptaethoxyethyl alcohol ($C_{12}EO_8$) on silica [44].

surfactant concentration, molecular structure (EO number and hydrocarbon chain length), temperature and electrolyte. In contrast to EO surfactants, sugar-based surfactants form a novel class of environmentally benign nonionic species [48,49]. Interestingly, while EO surfactants adsorb strongly on silica but not on alumina [50], sugar-based *n*-dodecyl-β-D-maltoside is found to adsorb on alumina, titania, and hematite but weakly on silica [17,49,51]. The EO groups are considered [44] to be unable to disrupt the rigid water layer surrounding the alumina substrate and the EO–Al^{3+} complexes stable relative to EO in the surface-adsorbed state. *N*-dodecyl-β-D-maltoside is found to be slightly acidic in nature [48] and hence it does not adsorb on silica at pH above its IEP of ~2.

Adsorption of polyethylene glycol on silica is high at low pH but reduces with increase in pH as a result of a decrease in silanol groups at silica/solution interface at higher pH. *N*-dodecyl-β-D-maltoside adsorption strongly depends on pH, where the adsorption increases with pH and reaches saturation at pH above 5–6 [52]. The adsorption of the nonionic surfactants also depends on the number of the hydrophilic groups and the hydrocarbon chain length. For polyethylene glycols of the same hydrocarbon chain length, the area occupied per ethylene glycol group increases with the number of ethylene glycols, ranging from 4.6 $Å^2$ at $m=2$ (m is the number of ethylene glycols in C_nEO_m) to 10.4 $Å^2$ at $m=40$ [53–55]. The saturation adsorption density is lower for molecules with a high degree of ethoxylation because of the increase in the packing area of each molecule on the solid surface with the degree of ethoxylation. Similarly, the degree of polymerization of sugar-based head group also determines its saturation adsorption density [56,57]. In contrast, the alkyl chain affects only the onset of saturation adsorption for both polyethylene and sugar-based surfactants.

The nonionic surfactant/solid systems in the literature are tabulated in Table 2 [62,65,66].

3.4. Adsorption of zwitterionic and gemini surfactants

The adsorption mechanism of zwitterionic surfactants such as C12 and C14 homologues of (alkyldimethylammonio) ethanoate and (alkyldimethylammonio)-1-propane sulfonate has been proposed to involve an interplay of the hydrophobic interaction and ion–dipole interaction between the charged groups at the solid/solution surface and the zwitterionic part [68].

Alami and Holmberg have reviewed recent work on the adsorption of hetero-gemini surfactants at silica/solution interface [69]. Optical reflectometric results suggest that the adsorption density of non-ionic hydroxyl group and methyl-capped poly(ethylene glycol) surfactant on hydrophilic silica is twice that on hydrophobic silica but less than that of its homologue due to the steric hindrance of the hetero-gemini surfactant. On the other hand, the adsorption of sulfate and a polyoxyethylene hetero-gemini surfactant decreases with an increase in the degree of ethoxylation. However, the packing of this surfactant is not as compact as that of the nonionic hetero-gemini surfactant.

3.5. Models for adsorption of single surfactants on solids

An adsorption isotherm can be classified basically into three types according to its shape: Langmuir type (L-type), S-type and "double plateau" type (L–S type). While the L-type adsorption can be represented by the simple Langmuir equation [70], the mechanisms of S and L–S types [71] are complex. The

Table 2
List of adsorption systems of nonionic surfactants

Surfactant	Type	Solid	Technique	Reference
n-Dodecyl-beta-D-maltoside	Nonionic	Silica, alumina, titania, hematite, graphite		[50]
n-Dodecyl-beta-D-maltoside	Nonionic	Alumina	Adsorption, zeta potential, surface tension, conductivity	[52]
n-Dodecyl-beta-D-maltoside	Nonionic	Hematite	IR	[53]
Glucoside, maltoside	Nonionic	Alumina		[58]
n-alkyl-beta-D-glucosides	Nonionic	Titania, silica	Ellipsometry	[59]
Alkyl polyglucosides	Nonionic	Titania	Rheology, adsorption, zeta potential	[49]
NP-10,15,20, OP-10,30	Nonionic	Silica	Fluorescence, adsorption	[55]
	Nonionic			[60]
CnEm	Nonionic	Graphite, hydrophilic silica and hyrophobic silica	AFM	[61]
CnE6 (n=10, 12, 14, 16)	Nonionic	Silica	Ellipsometry	[62]
C12Em, m=4,6,8−16	Nonionic	Silica	Adsorption, HPLC	[56]
CnEm	Nonionic	Silica		[51]
	Nonionic	Silicon	Neutron reflectivity	[63]
CnEm, NP, OP	Nonionic	Silica		[57]
C16E6	Nonionic	Silica	Neutron reflectivity	[64]
C12E6	Nonionic	Silica	Neutron reflectivity	[65]
C12E6	Nonionic	Silica	Small angle neutron scattering	[66]
C12E6, C12E8, C16E6, C16E8	Nonionic	Silica	Small angle neutron scattering	[67]
Octa(oxyethylene) Monododecyl ether	Nonionic	Silica	HPLC	[68]
Triton X-100	Nonionic	Silica	Small angle neutron scattering	[69]

thermodynamic model proposed by us [5] considered the electrostatic and hydrophobic lateral interactions as the major driving forces for the adsorption of ionic surfactants on the negatively charged surface with,

$$\Delta\overline{G^0_{ads}} = \Delta G^0_{\text{elec}} + \Delta G^0_{\text{hyd}} = -zF\psi_\delta/RT - n\phi/RT \tag{6}$$

where ψ_δ is the potential in the δ and ϕ is the energy for transfer of each $-CH_2$. These two parameters can be obtained from zeta potential and critical solloid (hemi-micelle) concentration (CSC) measurements, respectively. This particular model [5] can simulate the adsorption isotherm up to the maximum adsorption density.

A thermodynamic model has been formulated, based on "two-dimensional condensation" theory [72], similar to the "pseudophase separation model", taking into consideration the normal potential energies as well as the surface heterogeneity. Later approaches considered the two-dimensional adsorbed structures coexisting with monomers, monolayer and bilayers at the solid/solution interface in the presence of the "excluded volume" effect [73,74]. Johnson and Nagarajan [75] predicted the nanostructure of cationic and nonionic surface aggregates by comparing the equilibrium free energies for different structures such as spheres, cylinders, and monolayers covered with hemisphere, hemicylinder, finite disk and bilayer. This model can predict the solution concentrations where the surface aggregates transform from one structure to another. In addition to the above, the thermodynamics of the surface aggregation at the solid/solution interface in equilibrium with the bulk solution has been considered by Levitz using the grand partition function [76]. Another set of work applied the self-consistent field lattice (SCFL) theory [77–80] originally developed by Scheutjens and Fleer [77] for polymer adsorption.

The above models are either very complex (several equations with an input of four or more parameters) or are limited to only one type of adsorption isotherm. In contrast to the above, Gu and Zhu [81] developed two models for L, S and L–S type isotherms in which the adsorption process was treated as reactions between unoccupied sites and surfactant molecules. One is called a "one-step" model and the other a "two-step" model.

In the one-step model, the surfactant monomer interacts with the active site to form a solloid (hemi-micelle) as below:

$$\text{Site} + \text{Monomer} \rightleftarrows \text{Hemi} - \text{micelle}$$

and the equilibrium constant of this reaction is given by

$$k = a_{\text{hm}}/a_{\text{s}}a \tag{7}$$

where a_{hm}, a_{s} and a are the activities of adsorbed hemi-micelle, surface site, and surfactant monomer, respectively. It should be noted that a is equal to surfactant concentration C at low concentrations. The activities can be converted to adsorption density (Γ) through mass action law and then the final equation is:

$$\frac{\Gamma}{\Gamma_\infty - \Gamma} = kC^n \tag{8}$$

where Γ_∞ is the maximum adsorption density at high solution concentrations, C is the surfactant concentration in solution and n is the aggregation number.

The two-step model is a modified one-step model by considering the adsorption process to occur in two steps. In the first step, surfactants monomers adsorb on the solid surface at concentrations below the critical aggregation concentration (cac), thus no aggregates form.

$$\text{Site} + \text{Monomer} \rightleftarrows \text{Adsorbed Monomer}$$

And in the second step, the adsorbed surfactant monomers act as anchors for the formation of hemi-micelle:

$$(n-1)\text{Monomers} + \text{Adsorbed Monomer} \equiv \text{Hemi} - \text{micelle}$$

The general expression for the two-step model is as below:

$$\Gamma = \frac{\Gamma_\infty k_1 C\left(\frac{1}{n} + k_2 C^{n-1}\right)}{1 + k_1 C(1 + k_2 C^{n-1})} \tag{9}$$

where the k_1 and k_2 are the equilibrium constants for the first and second reactions, respectively.

Compared to the model proposed by us, where the free energies are measured experimentally, the one-step and two-step models extract information, such as aggregation number and equilibrium constant, from the adsorption isotherms. Then the standard free energy for surface aggregation (ΔG^0_{sa}) is calculated using the equation:

$$\Delta G^0_{\text{sa}} = -(1/n)RT\ln k \tag{10}$$

where R is the gas constant and T is the absolute temperature.

The standard free energy for solloidal hemi-micellization can be compared to that for micellization:

$$\Delta G^0_{\text{mic}} = -RT\ln(\text{cmc}) \tag{11}$$

If $\Delta G^0_{\text{sa}} < \Delta G^0_{\text{mic}}$, the surface aggregation is energetically favored.

From ΔG^0_{hm}, both the standard entropy (ΔS^0_{hm}) and the standard enthalpy (ΔH^0_{hm}) of solloidal hemi-micellization can be obtained using the equations:

$$\Delta S^0_{\text{hm}} = -\frac{\partial\left(\Delta G^0_{\text{hm}}\right)}{\partial T} \tag{12}$$

and

$$\Delta H^0_{\text{hm}} = \Delta G^0_{\text{hm}} + T\Delta S^0_{\text{hm}} \tag{13}$$

Although the aggregation number n obtained from the models is smaller than that measured using spectroscopic methods, the values for ionic and nonionic surfactants are comparable [82].

3.6. Nanostructures of surfactant aggregates

The structure of adsorbed aggregates at a molecular level is largely unknown to date. As mentioned before, based on wettability, electrokinetic and coagulation experiments, adsorbed

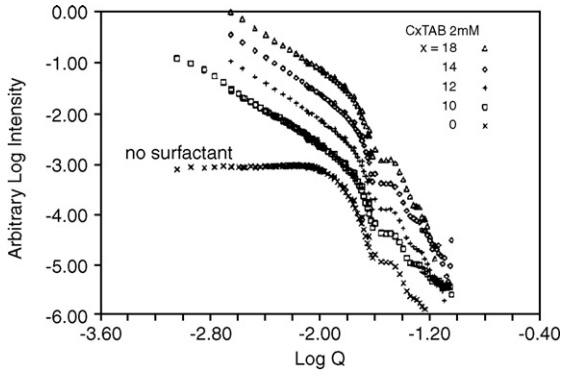

Fig. 6. Scattering spectra of silica (diameter of 38 nm) aggregates made with trimethylammonium bromide alkanes (C_xTAB), 2×10^{-3} M, with number of tail carbons x as follows: triangles, $x=16$; diamonds, $x=14$; pluses, $x=12$; squares, $x=10$; crosses, scattering of silica sphere in the absence of surfactant) for comparison [41].

surfactant aggregates on mineral solids have been proposed to be in the form of hemi-micelles [7,83,84]. Direct imaging using atomic force microscopy (AFM) surfactant concentrations above half of the cmc has recently shown that the structures of aggregates of nonionic ethoxylated or cationic surfactants on silica sometimes are similar to morphologies of bulk micelles and that the surface aggregates undergo sphere to cylinder transition with increase in surfactant concentration [59,85–87]. Although a majority of results from ellipsometry [60], small angle neutron scattering [64] and neutron reflectivity [61] suggested that nonionic ethoxylated and cationic surfactant aggregates exist in the form of patchy or fully covered bilayers, a few exceptions [88,67] have been noted using the same techniques. For example, Schulz et al. developed a model [88] for the micelle-like aggregates by analyzing neutron reflectivity data and then Oberdisse [67] determined the nanostructures of Triton X-100 on silica nano-particles at maximal surface coverage to be like those of micelles using small angle neutron scattering technique.

We have used SANS to determine the stability of colloidal suspensions [89]. Addition of calcium chloride ($CaCl_2$) to negatively charged silica spheres resulted in fractal coagulation. Unlike the fractal aggregates (diffusion-controlled, cluster–cluster aggregates), the aggregation of silica spheres exhibited both fractal and non-fractal behaviors in the presence of cationic alkyltrimethylammonium bromides [41]. Study of the effects of concentration and structure of surfactant molecules showed a significant and systematic increase in the apparent fractal dimension with an increase in the concentration of cationic single chain alkyltrimethylammonium bromide surfactants and reordering to a liquid-like structure and redispersion with a double chain cationic surfactant. The pattern of the scattering spectrum was not found to change as a function of the hydrophobic chain length as shown in Fig. 6. This suggested that the property governing the structure was charge neutralization, and not hydrophobic interaction.

In addition to the techniques discussed above, spectroscopic techniques such as fluorescence, electron spin resonance, Fourier transform infrared, excited-state resonance Raman have been employed to obtain information on the structure of the adsorbed surfactant layers. These techniques used recently for examining the aggregates at the solid/solution interface are reviewed below.

3.6.1. Fluorescence spectroscopy

Fluorescence emission depends on the environment of the light absorbing species and it has been used for exploring the solution behavior of surfactants. The fluorescence measurements are generally carried out by a steady state fluorescence spectrofluorometer and time resolved fluorescence lifetime instruments. We have adopted this technique to investigate the nano-structures of adsorbed layers at the solid surfaces and to obtain information on the polarity and viscosity of the interior of the adsorbed layer as well as the aggregation number of the surfactant solloids at the solid/solution interface.

For example, the adsorption of sodium dodecyl sulfate on alumina has been studied using fluorescence to investigate various stages in the adsorption process (Fig. 4) [84]. In steady state fluorescence spectroscopy, the ratio of relative intensities of the third peak to the first peak, I_3/I_1, in a pyrene emission spectrum shows the greatest solvent dependency. This ratio increases as the polarity decreases and hence can be used to estimate the solvent polarity of an unknown nanoenvironment in which the pyrene probe is located. I_3/I_1 values for pyrene were determined for alumina–SDS/water systems for various regions of the adsorption isotherm. The results are shown in Fig. 7, which is marked by an abrupt change in the local polarity of the probe from an aqueous environment to a relatively nonpolar micelle-type environment. This abrupt change occurs in a region

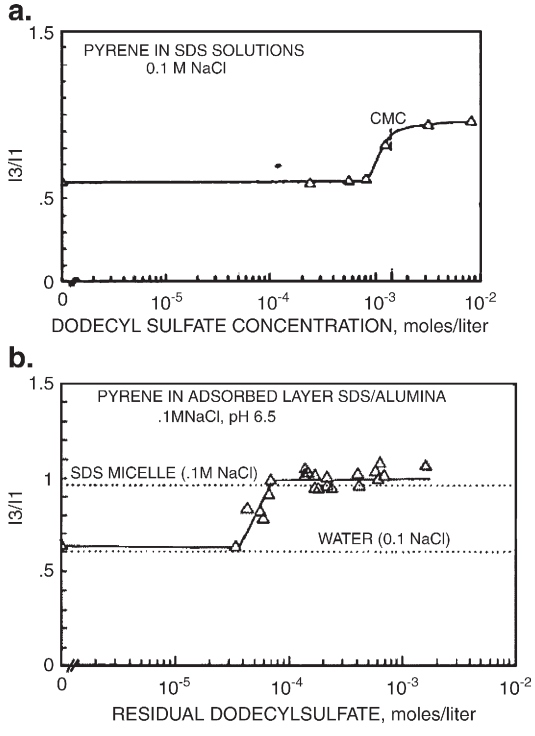

Fig. 7. (a) I_3/I_1 fluorescence parameter of pyrene in sodium dodecyl sulfate solutions in 0.1 M NaCl ($I_3=383$ nm, $I_1=374$ nm). (b) I_3/I_1 fluorescence parameter of pyrene in SDS/alumina slurries [84].

that is well below the cmc and approximately coincides with the transition in the adsorption isotherm from region I to II. In the plateau region, the I_3/I_1 value coincides with the maximum I_3/I_1 value for SDS solutions (Fig. 7), indicating the completion of aggregation on the surface. Thus, fluorescence studies provide a means to detect the formation of hydrophobic nanodomains at the interface and to determine the properties of such domains.

In the fluorescence lifetime method, when a fluorescence probe is excited by a short nanosecond pulse of light, its decay is enhanced in the presence of molecules that act as quenchers. The lifetime of the probe under quenching conditions would be determined by the concentrations of both the quencher and the probe as well as by the rate at which they diffuse and encounter each other. Kinetic analysis of the fluorescence decay profiles can, therefore, provide information on the local concentration of the reactants and hence the size of the local aggregates.

A kinetic analysis, based on this relation, carried out from the decay profiles of pyrene in the adsorbed layer of SDS at alumina/solution interface gives information on the evolution of the structure of the adsorbed layer. The SDS aggregation numbers obtained are marked on the adsorption isotherm in Fig. 8. The aggregates in region II appear to be of relatively uniform size (120 to 130), but in region III there is a marked growth in the aggregate size (160 to 360). Region II and above are characterized by surfactant aggregates of limited size. Further adsorption occurs mainly by the increase in the number of aggregates as revealed by a near constant aggregation number around 360. The transition from region II to III corresponds to the isoelectric point of the solid, and adsorption in region III occurs through the growth of existing aggregates rather than by the formation of new ones, suggesting that the aggregates possibly change from a patchy monolayer (head facing alumina) to a patchy bilayer (one head facing solution, the other facing the alumina). Such a situation with a reverse orientation of the surfactant molecules is illustrated in Fig. 9, where the whole process of adsorption has been schematically portrayed. These

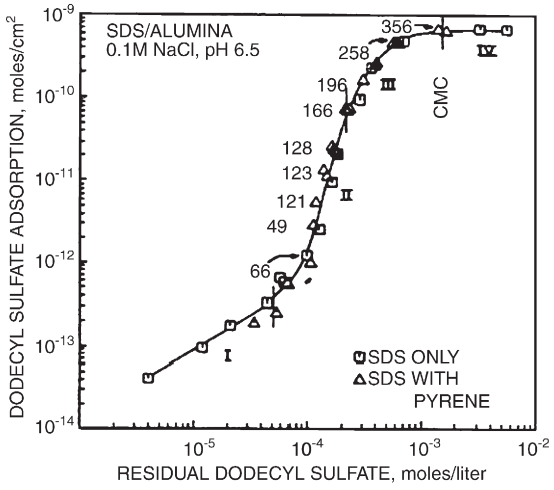

Fig. 8. Surfactant aggregation numbers determined at various adsorption densities along alumina/SDS system [84].

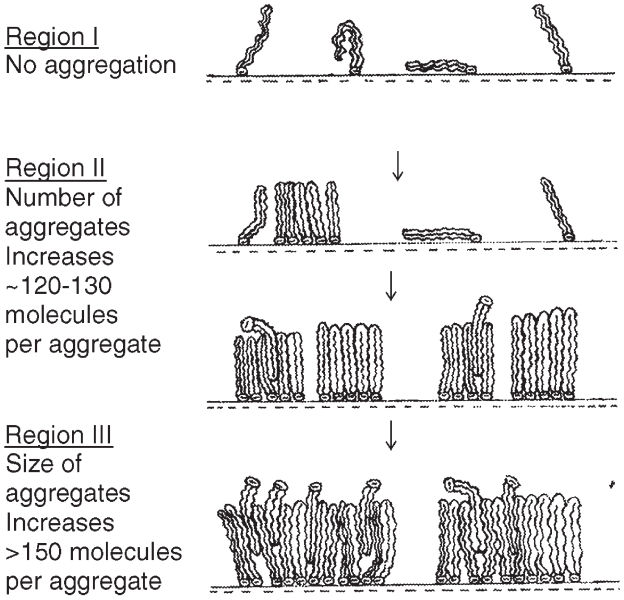

Fig. 9. Schematic representation of the correlation of the growth of aggregates for various regions of the adsorption isotherm depicted in Fig. 4 [84].

studies on the adsorbed layer of SDS on alumina reveal in detail the mechanism of adsorption of surfactants on solids.

3.6.2. Electron spin resonance (ESR)

The electron spin resonance spectroscopic technique uses transitions induced between Zeeman levels of a paramagnetic system situated in a static magnetic field. Species with a magnetic moment are capable of interacting with the magnetic field and give characteristic spectra.

For the study of SDS adsorption on alumina, nitroxide spin labels were chosen as the electron spin resonance probes. These spin labels (in μmol levels) were coadsorbed individually on alumina with sodium dodecyl sulfate [38]. As shown in Fig. 10, the shape of the adsorption isotherm of SDS on alumina with the probe is similar to that in the absence of the probe, except at low SDS concentrations where an enhancement in SDS adsorption is observed due to the synergistic co-adsorption of the surfactant with the probe. The ESR spectrum of 16-doxylstearic acid probe in aqueous solution shows the typical isotropic three-line spectrum characteristic of the nitroxide. The spectra obtained from the alumina/solution interface, on the other hand, are distinctly different from the solution spectrum, with three types of ESR spectra. At low SDS concentrations ($<1.5\times10^{-4}$ M), the probe aggregates strongly on the surface, leading to a spin-exchange narrowed spectrum consisting of a single broad peak (Fig. 10, curve A). As the SDS concentration is raised sufficiently to allow significant SDS hemi-micellar solloid formation at the interface, a sharper anisotropic spectrum is obtained. In this region, SDS solloid formation leads to a breakup of the surface aggregates of the probe. Individual nitroxide probe then no longer interacts strongly enough with other nitroxide probes to result in narrowing of the spectrum, and the spectrum obtained is anisotropic due to the high local viscosity. A calibration curve of relative rotational correlation times of 16-doxylstearic acid probe in mixtures of ethanol–glycerol (Fig. 11) shows that the solloid spectrum is

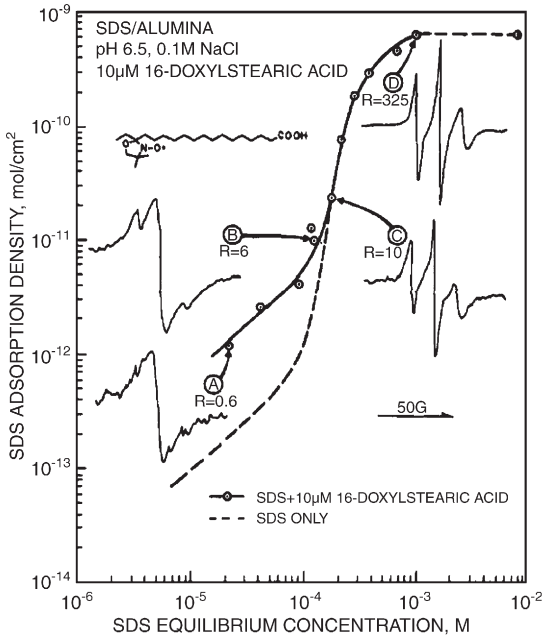

Fig. 10. ESR spectra of 16-doxylstearic acid in SDS surface aggregates at alumina/solution interface in various regions of the adsorption isotherm. Here, spectrum A corresponds to monomer adsorption; spectra B and C reflect adsorption of aggregates while spectrum D shows the saturation of adsorption [37].

similar to that obtained in 75–80% glycerol. At higher SDS concentrations, the spectrum remains essentially unchanged (Fig. 10, curve D). This suggests that the aggregate structure does not change appreciably as a function of SDS surface coverage. ESR spectroscopy with nitroxide spin probe is thus a useful method for probing the nanoenvironments of surfactant aggregates at solid/solution interface.

3.6.3. Raman spectroscopy

Unlike fluorescence spectroscopy and electron spin resonance, which depend on the use of an externally added or labeled luminescent and free radical bearing moieties that could cause perturbation to the environment around the probe, infrared and Raman spectroscopies are intrinsic techniques that can probe the system without any disturbance. Raman spectroscopy has an edge over the infrared absorption spectroscopy in that the sample handling is easy and the spectrum covers a wide range (50–5000 cm^{-1}).

Raman spectroscopy is essentially a scattering technique providing information on the vibrational modes of a molecule. Those vibrations cause a polarizability change of a Raman-active molecule. Importantly, the Raman spectroscopic analysis of surfactant aggregates has yielded information on the relative orientation of alkyl chains of the surfactant. Excited state Raman spectra of $Ru(bpy)_3^{2+}$ in micelles and in the adsorbed SDS layers on alumina in situ have shown that several transitions are sensitive to the evolution of the nanostructure of solloids [39] and that the surfactant adsorbs with reverse orientation (ionic heads facing the bulk solution) in the final stages of the adsorption and that the surface then becomes hydrophilic.

4. Adsorption of surfactant mixtures

Adsorption of surfactant mixtures [90] has received particular attention since commercial surfactant systems are generally mixtures of surfactants with various hydrophobic and polar groups. Interactions between surfactants in mixtures can produce marked interfacial effects due to change in adsorption as well as in the charge density of the surface. A typical feature of the adsorption of ionic–nonionic mixtures is the synergy or antagonism at interfaces [91,92]. In particular, the adsorption of one surfactant is often enhanced by the addition of a small amount of the other through hydrophobic interactions. The interactions between surfactant mixtures at solid/solution interface and in solution are described below for several systems.

4.1. Anionic–cationic surfactant mixtures

As mixtures of cationic and anionic surfactants tend to form precipitates, a few studies of adsorption of cationic and anionic surfactants on silica can be found in the literature [93]. Also in the case of cationic and anionic surfactants on silica, Gu and coworkers [93] have found that the adsorption of both cationic and anionic surfactants on silica can be promoted by co-adsorption of cationic surfactants.

4.2. Anionic–nonionic surfactant mixtures

For anionic–nonionic surfactant mixtures, we studied the system of dodecyl sulfate/sulfonate as the anionic surfactant and polyoxyethylene glycol and sugar-based surfactant as the nonionic components.

In the case of anionic–nonionic surfactant mixtures, they do not usually adsorb themselves but co-adsorb in the presence of another component. For example, only the anionic sodium *p*-octylbenzene sulfonate adsorbs on alumina while the nonionic $C_{12}EO_8$ does not [90]. The adsorption densities of both the sodium *p*-octylbenzene sulfonate and the $C_{12}EO_8$ are promoted in the mixture. The adsorption density has been correlated with

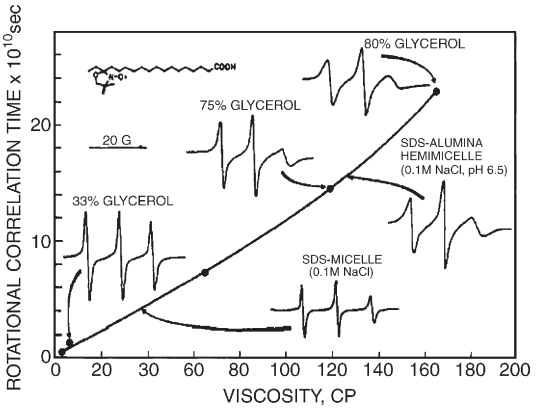

Fig. 11. Comparison of ESR spectra of 16-doxylstearic acid in surface aggregate, micelles, and ethanol–glycerol mixtures and corresponding rotational correlation times [37].

the solution concentration of the surfactant monomer for various mixed systems [90,94,95]. The cac (critical aggregation concentration) value of the mixture is often lower than those of individual components. The aggregation number of the surface aggregates determined for the mixed system (of sodium dodecyl sulfate and octyl ethoxylated dodecyl ether ($C_{12}EO_8$)) using fluorescence [92] showed a higher aggregation number for mixed aggregates than those of the components. Also, when $C_{12}EO_8$ adsorbs, the floatability of kaolin in the mixed systems is less than that in sodium dodecyl sulfate solutions, suggesting the orientation of EO groups to be towards the bulk solution. The synergistic adsorption is attributed to the hydrophobic interaction between the two surfactants as well as the reduction of the electrostatic repulsion between the anionic head group by the nonionic surfactant [91]. The role of the hydrocarbon chain length in the enhancement of adsorption of mixtures has been investigated using mixed systems of sodium dodecyl sulfate and polyoxyethylene glycols of different hydrocarbon chain lengths and kaolin. The adsorption isotherm of sodium dodecyl sulfate was found to remain unchanged if the hydrocarbon chain length of the polyoxyethylene glycol was equal or longer than that of the anionic surfactant; otherwise the isotherm of sodium dodecyl sulfate was altered, suggesting the effect of the asymmetry of the hydrocarbon chain on the adsorption of mixtures. In the case of sodium dodecyl sulfate and $C_{12}EO_8$ system on kaolin [92], the adsorption density of the latter in region IV of the isotherm (plateau region) exhibits a maximum at the equimolar ratio of the two surfactants. This is attributed to the compact structure of the mixed aggregate at this particular mixing ratio. Treiner and coworkers observed that the desorption of both sodium dodecyl sulfate and $C_{12}EO_7$ from silica surface occurred at solution concentrations above 100 times of the cmc at pH 5 [96], although in this case, sodium dodecyl sulfate was incorporated into $C_{12}EO_7$ surface aggregates at lower concentrations. This is accounted for by considering the competition between mixed micelles in solution and at solid/solution interface for the surfactant molecules as well as the electrostatic repulsion between the silanol groups at the solid surface and anionic charged groups. The adsorption of $C_{10}E_5$ is inhibited greatly by the addition of the second component in the case of a binary surfactant mixture of asymmetrical hydrocarbon chain lengths of sodium dodecyl sulfate and $C_{10}E_5$ on silica at pH 6 [94]. The desorption is proposed to be due to the preference of surfactant molecules for mixed micelles than for surface aggregates.

Another anionic/nonionic surfactant system of interest is that involving sugar-based type. For example, in the case of co-adsorption of anionic sodium dodecyl sulfate and nonionic sugar-based *n*-dodecyl-β-D-maltoside (DM) on alumina [97], it was found that either synergy or antagonism could occur at solid–liquid interfaces, depending on the solution conditions. At pH 6 where alumina is positively charged, significant synergy between the two surfactants was observed in 0.03 M NaCl, especially at equimolar mixing ratio. The adsorption isotherms of the individual surfactants and their mixtures on alumina at pH 6 in 0.03 M NaCl are presented in Fig. 12. It can be seen that the adsorption density of the mixture in the saturation stage IV is more than that of *n*-dodecyl-β-D-maltoside itself. At pH 11 where alumina is negatively charged, SDS on the other hand exhibits an antagonistic effect on DM adsorption. It is noted that the composition of the surface aggregate varies as a function of both the surfactant bulk concentration as well as the overall surfactant mixing ratio, as shown in Fig. 13.

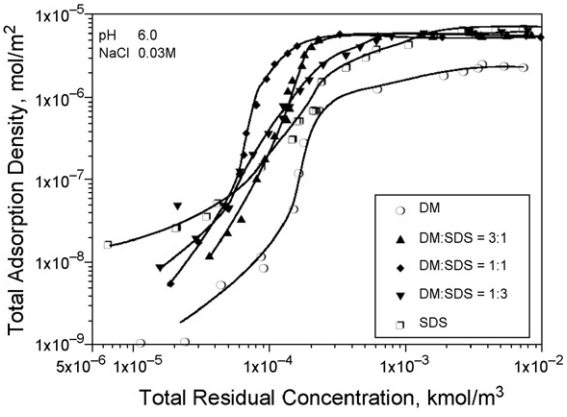

Fig. 12. Adsorption of dodecyl maltoside (DM), sodium dodecyl sulfate (SDS) and dodecyl maltoside/sodium dodecyl sulfate mixtures on alumina at pH 6 and 25 °C in 0.03 M NaCl solution [97].

4.3. Cationic–nonionic surfactant mixtures

The cationic–nonionic surfactant mixtures studied in detail include alkyl trimethyl chloride/bromide as the cationic and polyoxyethylene glycol or sugar-based surfactant as the nonionic surfactant.

4.3.1. Mixtures of cationic alkyltrimethyl chloride/bromide and polyoxyethylene glycol surfactants

Similar to anionic and nonionic surfactant mixtures, the adsorption of $C_{12}EO_8$ on hydrophilic solids at pH 5 and at 25 °C in 0.03 M NaCl is enhanced by the presence of dodecyltrimethylammonium chloride [98]. The mechanism for the co-adsorption of the cationic–nonionic surfactant mixtures is considered to be the same as that for the anionic–nonionic surfactant mixtures: hydrophobic interaction and the reduction of the electrostatic repulsion between the cationic head groups by the nonionic surfactant. Significant synergy has also been observed to exist in the cationic tetradecyl trimethylammonium chloride/nonionic pentadecylethoxylated nonyl phenol (NP-15) system on alumina at pH 10 (Fig. 14) [99]. The adsorption behavior is dependent on the composition of the surfactant mixture and the order of addition. Although NP-15 shows only trace adsorption on alumina, mixed adsorption is promoted with an increase in the cationic surfactant content of the mixture. It is to be noted that the total adsorption density was higher if the surfactants were premixed than that if the cationic surfactant was pre-adsorbed. Importantly, monomer concentrations of surfactant mixtures [100] calculated from the regular solution theory fail to agree with those obtained from the experiments. To account for the results obtained, a schematic

model involving two different mixed micellar species coexisting in solutions above the cmc has been proposed [101]. The model has been further developed to explain the coexistence of two micellar species in solution in terms of the packing parameter [102].

4.3.2. Mixtures of cationic dodecyltrimethylammonium bromide and sugar-based n-dodecyl-β-D-maltoside surfactants

In the mixed system of dodecyltrimethylammonium bromide (DTAB) and *n*-dodecyl-β-D-maltoside (DM) [103], the latter is co-adsorbed by the former (DM does not adsorb on silica by itself at pH 7) but dodecyltrimethylammonium bromide acts as an anchor molecule for DM in the case of mixed adsorption. When the surface is not saturated, adsorption of DTAB is enhanced by the DM. However, when the surface is saturated, the adsorption of DTAB is reduced due to the competition from DM. Interestingly, the ratio of DM/DTAB in the surface aggregate is found to be a function of the adsorption density and the solution concentration: the ratio starts at a low value at low concentrations and increases sharply at the critical aggregation concentration, reaches a maximum at the onset of the plateau region, and then decreases. Clearly the interaction between DM and DTAB is synergistic.

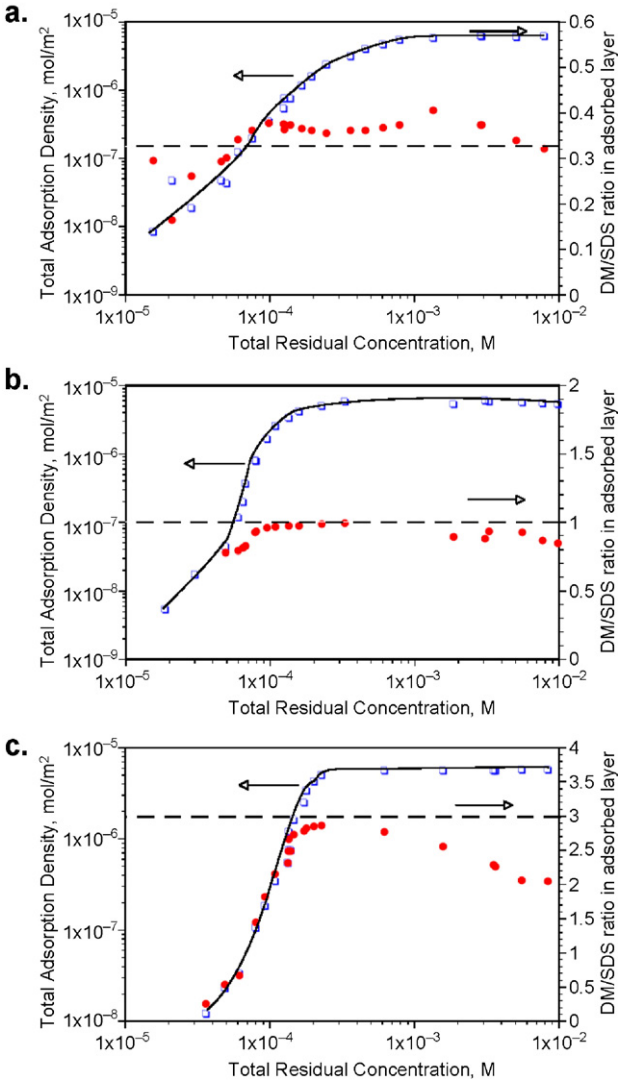

Fig. 13. Adsorption of dodecyl maltoside (DM)/sodium dodecyl sulfate (SDS) mixtures (squares, left *y* scale) and the DM/SDS ratios (circles, right *y* scale) in the surface aggregates. The dotted lines indicate the overall ratio of DM/SDS in the solution and at the solid/solution interface: (A) 1:3; (B) 1:1; (C) 3:1 [97].

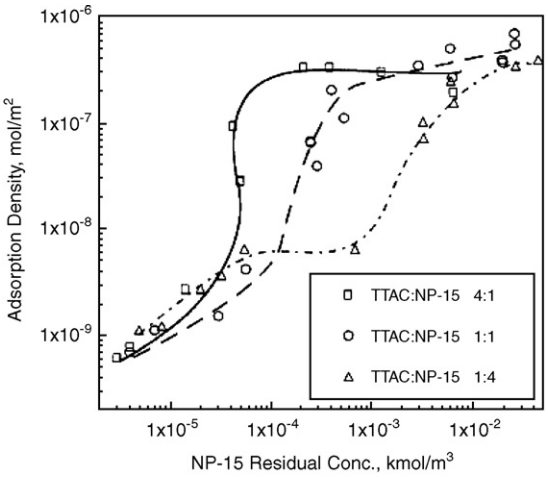

Fig. 14. Adsorption of pentadecylethoxylatednonyl phenol (NP-15) on alumina in the presence of varying amounts of tetradecyltrimethylammonium chloride (TTAC). pH 10, ionic strength 0.03 M NaCl [101].

4.4. Cationic–zwitterionic surfactant mixture

Locker and Ducker measured the force between borosilicate glass surfaces in mixed solutions of cationic dodecylpyridinium chloride and zwitterionic *N*-dodecyl-*N,N*-dimethyl-3-ammonio-1-propanesulfonate in 1 mM KCl in D_2O using AFM and

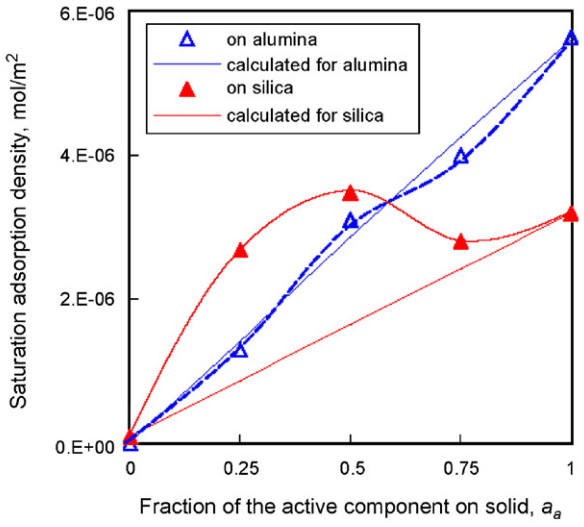

Fig. 15. Saturation adsorption density as a function of the surface fraction of the active component a_a. The solid and open triangles are the experimental data for the adsorption of mixtures on silica and alumina, respectively. The solid and dashed lines are the calculated results for the adsorption of mixtures on silica and alumina, respectively [108].

ATR-IR techniques [104]. The zwitterionic surfactant adsorbs very little by itself on the glass and has little effect on the force between the glass surfaces while a trace of cationic surfactant promotes the adsorption of the zwitterionic surfactant. The mechanism may involve the electrostatic and hydrophobic interactions.

4.5. Nonionic–nonionic surfactant mixtures

Nonionic–nonionic surfactant mixtures studied include mixtures of homologues of polyoxyethylene glycols and sugar-based surfactants.

4.5.1. Mixtures of homologues of polyoxyethylene glycols

Brinck and Tiberg [95] explored the effects of the hydrocarbon chain length and the degree of ethoxylation on the adsorption of mixtures of $C_{14}EO_6$–$C_{10}EO_6$ and $C_{12}E_5$–$C_{12}EO_8$ on silica. While the difference in the hydrocarbon chain lengths does affect the mixed cmc, the degree of ethoxylation does not make any difference in the adsorption of the mixture. Treiner and coworkers investigated the solution and adsorption behaviors of mixtures of $C_{14}EO_6$ and $C_{10}EO_6$ [105]. Depending on the solution composition, the mixture exhibits partial synergy and partial demixing in the solution, resulting in demixing at the silica/solution interface. The adsorption isotherm of $C_{14}EO_6$ is of S-shape while that of $C_{10}EO_6$ displays two plateaus in region IV. The surface aggregates have been proposed to be $C_{14}EO_6$-rich and $C_{10}EO_6$-rich.

4.5.2. Mixtures of polyoxyethylene glycol and sugar-based surfactants

4.5.2.1. Solution behavior. Mixtures of nonyl phenol ethoxylated decyl ether (NP-10) and *n*-dodecyl-β-D-maltoside (DM) exhibit demixing in aqueous solution [106] with two micellar species present in the NP-10-rich solution [107].

4.5.2.2. Prediction of structure of surface aggregates. Cooperative adsorption of nonionic surfactant mixtures of nonyl phenol ethoxylated decyl ether (NP-10) and *n*-dodecyl-β-D-maltoside (DM) has been investigated for silica and alumina systems [108]. In the case of adsorption of the mixed system on alumina, DM is identified to be the "active" component while nonyl phenol ethoxylated decyl ether is the "passive" one (coadsorbing only), while their roles are reversed for the adsorption on silica. At high solution concentrations where saturated adsorption is reached, the difference between the maximum adsorption of mixtures and those of individual components is related to the interaction between the components in the surface aggregates. If the adsorption density of a mixture is more than that of any individual component, synergy exists in the surface aggregation, otherwise antagonism occurs. Ideality corresponds to a situation where the adsorption density of a mixture follows a linear relationship between those of single surfactants as a function of the mixing ratio. Fig. 15 shows the maximum adsorption densities from the experiments and calculations as a function of the distribution of the active component on the solid surface (a_a). The experimental data for the mixtures on silica are always larger than the calculated values with a maximum at an equal molar mixing ratio, suggesting synergy. However, results from the experiments and calculations agree with each other for the adsorption on alumina, showing little synergy. The synergy between two different surfactant molecules is attributed to the dissimilarities between the bulk and surface aggregates due to the nature of packing of molecules of different structures.

To explain the synergy in the surface aggregation from a molecular structure point of view, the nanostructure of the mixed surface aggregate is estimated using a modified packing parameter which can be expressed as below [108]:

$$P_{\text{mix}} = \sum x_i P_i \tag{14}$$

$$P_{\text{mix}} = \sum x_i V_i / (a_0 \times l_i) \tag{15}$$

where the P_{mix} and P_i are the packing parameters [109] of mixed surface aggregates and of component i in the mixed surface aggregate, respectively. x_i, V_i, l_i are the mole fraction, volume and length, respectively, of the hydrocarbon chain for component i. In Eq. (15), a_0 is the average packing area at a composition obtained purely from the adsorption experiment.

The results from Eqs. (14) and (15) suggest that the nanostructure of mixed surface aggregates at silica/solution interface undergoes a sphere to cylinder transition. In the case of alumina/solution interface, while the aggregates are bilayers in the studied range, the values from Eq. (15) indicate a sphere to cylinder to bilayer transition.

To test the predictions from the two equations for the adsorption on alumina, the different nanostructures including sphere, hemisphere, spherical cylinder, hemispherical cylinder, and monolayer with hemisphere cap are compared with a fully occupied cube. The 3-D and side views of these nanostructures, as well as the filling ratio (V/V_{full}), are shown in Fig. 16. The filling ratio is defined as the volume of the nanostructure (V) over the volume of the occupied space (V_{full}).

Among all the nanostructures, the bilayer surfactant structure on hydrophilic solids can occupy the surface fully. Experimental data and packing parameters calculated using both Eqs. (14) and (15) suggest that the nanostructure of the surface aggregate of *n*-dodecyl-β-D-maltoside on alumina is "bilayer" type. As the maximum adsorption density of *n*-dodecyl-β-D-maltoside is proportional to V_{full} and that for the surfactant mixture is proportional to the V, the ratio of the adsorption density of the mixed aggregates over that for *n*-dodecyl-β-D-maltoside on alumina can be considered to be equal to V/V_{full}. The results show that the nanostructure is in good agreement with the packing parameters based on Eq. (15). The adsorption at 0.25 fraction of DM is less than 1/4 of that for *n*-dodecyl-β-D-maltoside, suggesting that the mixed aggregates form spheres or hemispheres, and this result also is in good agreement with those from Eq. (15). Hence, we conclude that the nanostructure of the mixed aggregate changes from the sphere to bilayer. The failure of

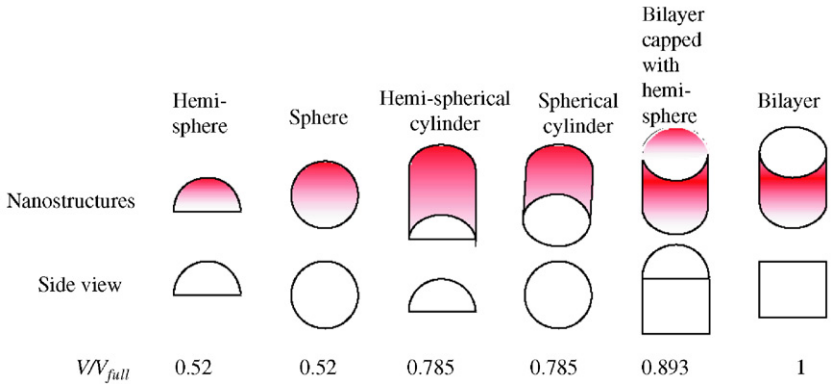

Fig. 16. 3-D and side views of various nanostructures together with the V/V_{full} ratio [108].

Eq. (14) is proposed to be due to the inappropriate values obtained for the cross-sectional area of the passive component nonyl phenol ethoxylated decyl ether at the air/liquid interface.

The molecular structures of *n*-dodecyl-β-D-maltoside and nonyl phenol ethoxylated decyl ether contribute towards the difference between the adsorption of mixtures on silica and alumina. These two molecules have similar lengths and volumes of hydrocarbon chains, but the hydrophilic group of nonyl phenol ethoxylated decyl ether is much longer (3.1 vs. 1.2 nm), larger (volume of 0.650 vs. 0.353 nm^3), and more flexible than that of *n*-dodecyl-β-D-maltoside. For the adsorption on silica, nonyl phenol ethoxylated decyl ether is the active component and *n*-dodecyl-β-D-maltoside is the passive one (can only co-adsorb). In this case, the packing area of nonyl phenol ethoxylated decyl ether (0.52 nm^2) is similar to that of passive *n*-dodecyl-β-D-maltoside (0.57 nm^2). Therefore, the adsorption of mixtures is not affected significantly by the difference in the sizes of their head groups. However, for the adsorption on alumina, the packing area of the active component *n*-dodecyl-β-D-maltoside (0.30 nm^2) is much smaller than that of passive nonyl phenol ethoxylated decyl ether (0.78 nm^2). Hence, the uptake of the passive component into the interfacial region results in a significant decrease in the total adsorption density of mixed adsorption as the available surface area of the solid remains the same.

4.5.2.3. Modeling of adsorption of surfactant mixtures. All the adsorption models to date are for single component systems [110]. There is clearly a need for a model for the adsorption of mixed surfactants. Kapur and Healy have considered adsorption of the homologues of nonionic surfactants using a parking lot model that essentially assumes an equilibrium between adsorption and desorption of each component and links the adsorption rate to the product of surfactant concentration in the solution and the available empty parking spaces on the solid surface [110].

A model is presented for the cooperative adsorption of surfactant mixtures where one component preferentially adsorbs on the solid while the other adsorbs very little by itself. Active components are those that are capable of adsorbing by themselves while passive ones are those that only co-adsorb with the assistance of the active ones. In this model, the active surface sites are considered to interact with n_a monomers of active adsorbing species *a* and n_p monomers of passive co-adsorbing species *p* to form surface aggregates. At equilibrium,

$$\text{Site} + n_a \text{ Monomer } a + n_p \text{ Monomer } p \rightleftarrows \text{Surface aggregates}$$

with *k* as the equilibrium constant for the reaction.

Applying mass action law, the adsorption can be expressed as:

$$\frac{\Gamma}{\Gamma_\infty - \Gamma} = kC^n \left(\frac{x_b^a}{1-x_b^a}\right)^{x_s^a n} (1-x_b^a)^n \tag{16}$$

where Γ and Γ_∞ are the adsorption densities at a certain concentration and the maximum adsorption density at high solution concentration, respectively. *C* is the total concentration, *n* the aggregation number, x_b^a and x_s^a are the mole fractions of the active component *a* in the bulk solution and in the surface aggregate, respectively.

Compared with Gu's model for single surfactants [81], Eq. (16) contains two more parameters for the micellization in solution and for aggregation at the solid/solution interface. At low concentrations, when no surface aggregate forms (n = 1), the above equation reduces to the Langmuir equation.

The data fitting for the system of nonyl phenol ethoxylated decyl ether (NP-10) and *n*-dodecyl-β-D-maltoside (DM) on silica and alumina has revealed that *n* is between 3 and 4 for the mixed adsorption on silica while it is 1 to 10 for that on alumina, possibly due to the variation in the type of nanostructures of the surface aggregates. Surface aggregation is the preferred process over micellization at $\Delta G_{sa}^0 < \Delta G_{mic}^0$. The values of ΔG_{sa}^0 and ΔG_{mic}^0 are $8.6RT$–$10.1RT$ (21.1–25.1 kJ/mol) and 8.5–$9.6RT$ (21.1–23.9 kJ/mol), respectively, which are typical for surfactants. Thus depending on the surfactant type and mixing ratio as well as the solid, there can be

important synergy or antagonism among different surfactant components.

In the above model, one single equation is used to present the adsorption of surfactant mixtures from which several parameters, such as aggregation number and the excess free energy for mixed adsorption, can be derived. This model is expected to apply to other systems composed of anionic/nonionic, cationic/nonionic and nonionic binary mixtures.

5. Summary

Adsorption of surfactants and their mixtures at solid/solution interface is a complex process. The driving force for adsorption is a combination of the electrostatic interaction, the chemical interaction, the lateral chain–chain associative interaction, the hydrogen bonding and desolvation of the adsorbate species. The adsorption of alkyl sulfates, alkyl sulfonates, alkyl amines and alkyl trimethylammonium salt surfactants has been reviewed here along with those of nonionic alkyl polyethylene glycol and sugar-based surfactants.

The adsorption isotherm of an ionic surfactant on an oppositely charged solid usually follows "Somasundaran–Fuerstenau" type, which is characterized by a four-stage mechanism: monomer adsorption through electrostatic interactions at low concentrations; surface aggregate formation through chain–chain associative interaction at concentrations above the critical aggregation concentration; bilayer formation with a reverse orientation of surfactant molecules at intermediate concentrations; and saturation adsorption at concentration above the cmc. Spectroscopic techniques, such as fluorescence, electron spin resonance (ESR) and Raman spectroscopies, as well as small angle neutron scattering, neutron reflectivity and atomic force microscopy, have been used to obtain information on nanostructural properties of the surface aggregates. Several mathematical models have also been introduced to represent different types of adsorption isotherms of surfactants and their mixtures.

Compared to the adsorption of single surfactants, adsorption of mixtures of anionic–cationic, anionic–nonionic, cationic–nonionic, cationic–zwitterionic and nonionic–nonionic types generally exhibit synergy at interfaces. Structures of mixed aggregates for nonionic surfactant mixtures have been predicted and a new model has been proposed to describe the adsorption of mixtures. A new packing parameter, $P_{mix}=\sum x_i V_i/(a_0 \times l_i)$, where the P_{mix} is the packing parameter of mixed surface aggregates. x_i, V_i, l_i are the mole fraction, volume and length, respectively, of hydrocarbon chain for component i. a_0 is the average packing area, is proposed for surfactant mixtures.

Acknowledgments

The support of this work by the Department of Energy (DE-FC26-01BC15312 and DE-FC26-03NT15413), the National Science Foundation EEC-0328614, and the industrial sponsors of the Industrial/University Cooperative Research Center (IUCRC) for advanced studies on novel surfactants at Columbia University is gratefully acknowledged.

Appendix A. List of symbols

a_{hm}	the activity of an adsorbed hemi-micelle
a_s	the activity of a surface site
a	the activity of the surfactant monomer
a_0	the average packing area of a hydrophilic group
A	cross-sectional parking area of a nitrogen molecule, 0.162 nm^2
A_{min}	minimum area per molecule at the interface, $Å^2$
C	the bulk or residual concentration of the surfactant
C_0	the total surfactant concentration before adsorption
cmc	critical micelle concentration
cac	critical aggregation concentration
F	the Faraday constant
g_i	mass of component i, g
ΔG^0_{ads}	the standard free energy of adsorption
ΔG^0_{elec}	the standard free energy of electrostatic interaction
ΔG^0_{chem}	the standard free energy of chemical interaction
ΔG^0_{c-c}	the standard free energy of chain–chain interaction
ΔG^0_{c-s}	the standard free energy of hydrophobic interaction
ΔG^0_{H}	the standard free energy of hydrogen bonding
$\Delta G^0_{H_2O}$	the standard free energy for desolvation
ΔG^0_{sa}	the standard free energy for surface aggregation
ΔG^0_{mic}	the standard free energy of micellization
ΔH^0_{hm}	the standard enthalpy of hemi-micellization
k	the equilibrium constant for aggregation at the interface
l_i	the length of hydrocarbon chain for component i
m	the mass of the solid in the suspension
N	Avogadro's constant
$n(CH_2)$	the number of CH_2 groups in the hydrocarbon chain
n_l	the number of layers of aggregate on solid, $n_l=1$ for monolayer and $n_l=2$ for bilayer
n	the aggregation number
P_{mix}	the packing parameter of mixed surface aggregates
P_i	the packing parameter of component i
$\tilde{r}$	the effective length of the chain
R	gas constant, 8.314 J mol^{-1} K^{-1}
ΔS^0_{hm}	the standard entropy of hemi-micellization
T	absolute temperature
V_i	the volume of hydrocarbon chain for component i
x_i	the mole fraction of component i
x^a_b	the mole fraction of the active component a in the bulk solution
x^a_s	the mole fraction of the active component a in the surface aggregate
z	the valency of the adsorbate species
Γ_{max}	the maximum adsorption density at interface, mol/m^2
Γ_δ	the adsorption density in the Stern plane δ, mol/m^2
$\Gamma_{max,solid}$	the saturation adsorption density at the solid/solution interface
$\Gamma_{max,air}$	the saturation adsorption density at the air/solution interface
Γ_∞	the maximum adsorption densities at high surfactant solution concentrations
ϕ	the energy gained per $-CH_2$ group
Ψ_δ	the potential in the Stern plane

References

[1] Xiao L, Xu G-Y, Zhang Z-Q, Wang Y-B, Li G-Z. Colloids Surf, A Physicochem Eng Asp 2003;224(1–3):199.
[2] Pethica BA. The contact angle equilibrium. J Colloid Interface Sci 1977;62:567.
[3] Sen Gupta AK, Papadopoulos KD. 203 (1998) 345.
[4] Wasan DT, Ginn M, Shah DO, editors. Surfactants in process engineering. New York: Marcel Dekker; 1988.
[5] Somasundaran P, Grieves RB, editors. Advances in interfacial phenomena of particulate/solution/gas systems. AIChE Symposium Series, 1975; 71 AIChE Symp. Ser. 71 (1975) 124.

[6] Fuerstenau DW. The adsorption of surfactants at solid/water interfaces. In: Hair ML, editor. The chemistry of biosurfaces, vol. 1. New York: Marcel Dekker; 1971. p. 143.
[7] Goddard ED, Somasundaran P. Croat Chem Acta 1976;48(4):451.
[8] Somasundaran P, Agar GE. J Colloid Interface Sci 1967;24:433.
[9] French RO, et al. J Phys Chem 1954;58:805.
[10] Peck AS, Wadsworth ME. Infrared studies of the effect of fluoride, sulfate and chloride on chemisorption of oleate on fluoride and barite. In: Arbiter N, editor. Proc. 7th Int'l Mineral Processing Congress; 1965. p. 259.
[11] Ananthapadmanabhan KP, Somasundaran P. Colloids Surf 1985;13:151.
[12] Gaudin AM, Fuerstenau DW. Trans AIME 1955:1–7.
[13] Fuerstenau DW, Healy TW, Somasundaran P. Trans AIME 1964;202:958.
[14] Somasundaran P, Kunjappu JT. Colloids Surf 1989;37:245.
[15] Lin IJ, Somasundaran P. J Colloid Interface Sci 1971;37(4):731.
[16] Doren A, Vargas D, Goldfrab J. Inst Min Metall Trans, Sect C, vol. 84; 1975. p. 34.
[17] Zhang L, Somasundaran P, Mielczarski J, Mielczarski E. J Colloid Interface Sci 2002;256:16.
[18] James RO, Healy TW. J Colloid Interface Sci 1972;40(1):65.
[19] Evenas L, Furo I, Stilbs P, Valiullin R. Langmuir 2002;18(21):8096.
[20] Kamyshny A, Lagerge S, Partyka S, Relkin P, Magdassi S. Langmuir 2001;17(26):8242.
[21] Rosen MJ. Surfactants and interfacial phenomena. 2nd ed. . New York: Wiley-Interscience; 1989.
[22] Koopal LK, Lee EM, Böhmer MR. J Colloid Interface Sci 1995;170:85.
[23] Somasundaran P, Fuerstenau DW. J Phys Chem 1966;70:90.
[24] Fan A-X, Somasundaran P, Turro NJ. Langmuir 1997;13:506.
[25] Trogus FJ, Schechter RS, Wade WH. J Colloid Interface Sci 1978;298: 70.
[26] Sexsmith FH, White HJ. J Colloid Interface Sci 1959;14:598.
[27] Paria S, Khilar KC. Adv Colloid Interface Sci 1994;110:75.
[28] Somasundaran P, Ananthapadmanabhan KP, Deo P. J Colloid Interface Sci 2005;290:357.
[29] Ananthapadmanabhan KP, Somasundaran P. Colloids Surf 1983;77: 105.
[30] Siracusa PA, Somasundaran P. J Colloid Interface Sci 1987;120:100.
[31] Sivakumar A, Somasundaran P, Trach S. J Colloid Interface Sci 1994;159:481.
Sivakumart A, Somasundaran P. Langmuir 1994;10(1):131.
[32] Viswanathan KV, Somasundaran P. Colloids Surf 1987;26:19.
[33] Fu E, Somasundaran P, Maltesh C. Colloids Surf, A Physicochem Eng Asp 1996;112:55.
[34] Somasundaran P, Ananthapadmanabhan KP, Viswanathan KV. Soc Pet Eng AIME, SPE 1983:97.
[35] Somasundaran P, Hanna HS. Soc Pet Eng J June 1985:343.
[36] Chia YH, Somasundaran P. Carrier flotation of anatase from clay and its physicochemical mechanisms. In: Malghan SG, editor. Ultrafine grinding and separation of industrial minerals. New York: AIME; 1983.
[37] Morgan LJ, Somasundaran P, Partyka S. Colloids Surf 1987;27:15.
[38] Waterman KC, Turro NJ, Chandar P, Somasundaran P. J Phys Chem 1986;90:6828.
[39] Kunjappu JT, Somasundaran P, Turro NJ. J Phys Chem 1990;94:8464.
[40] Ananthapadmanabhan KP, Somasundaran P, Healy TW. SME–AIME Trans 1979;265:2003.
[41] Wong K, Cabane B, Duplessix R, Somasundaran P. Langmuir 1989;5: 1346.
[42] Huang L, Somasundaran P. Colloids Surf, A Physicochem Eng Asp 1996;117:35.
[43] Trompette JL, Zajac J, Keh E, Partyka S. Langmuir 1994;10(3):812.
[44] Somasundaran P, Krishnakumar S. Colloid Surf, A 1997;123–124:491.
[45] Markowitz MA, Klaehn J, Hendel RA, Qadriq SB, Golledge SL, Castner DG, et al. J Phys Chem, B 2000;104:10820.
[46] Blin JL, Léonard A, Su BL. J Phys Chem, B 2001;105:6070.
[47] Pérez-Arévalo JF, Domínguez JM, Terrés E, Rojas-Hernández A, Miki M. Langmuir 2002;18(4):961.
[48] Smith GA, Zulli AL, Grieser MD, Counts MC. Colloids Surf, A 1994;88 (1):67.
[49] Zhang L, Somasundaran P, Maltesh C. J Colloid Interface Sci 1997;191: 202.
[50] Lawrence SA, Pilc JA, Readman JR, Sermon PA. J Chem Soc Chem Commun 1987:1035.
[51] Mielczarski E, Mielczarski JA, Zhang L, Somasundaran P. J Colloid Interface Sci 2004;275:403.
[52] Lu S, Somasundaran P, unpublished results.
[53] Misra PK, Mishra BK, Somasundaran P. J Colloid Interface Sci 2003;265:1.
[54] Desbène PL, Portet F, Treiner C. J Colloid Interface Sci 1997;190: 350.
[55] Partyka S, Zaini S, Lindheimer M, Brun B. Colloids Surf, A 1984;12 (3–4):255.
[56] Zhang L, Doctor of Engineering Science thesis, Columbia University, 1998.
[57] Matsson MK, Kronberg B, Claesson PM. Langmuir 2004;20(10):4051–8.
[58] Chai J, Li G, Zhang G, Zhang Y. Huaxue Tongbao 2002;65(8):506–15.
[59] Grant LM, Tiberg F, Ducker WA. J Phys Chem, B 1998;102:4288–94.
[60] Tiberg F, Jonsson B, Tang J, Lindman B. Langmuir 1994;10:2294–300.
[61] Thirtle PN, Li ZX, Thomas RK, Rennie AR, Satija SK, Sung LP. Langmuir 1997;13:5451–8.
[62] Penfold J, Staples E, Tucker I, Fragnetto G. Phys, B Condens Matter 1996;221(1–4):325–30.
[63] Penfold J, Staples E, Tucker I. Langmuir 2002;18(8):2967–70.
[64] Cummins PG, Penfold J, Staples E. J Phys Chem 1992;96(20):8092–4. Kline SR, Kaler EW. Langmuir 1992;12:2402.
[65] Penfold J, Staples E, Tucker I, Cummins P. J Phys Chem 1996;100 (46):18133.
[66] Rheinlander T, Klumpp E, Schlimper H, Schwuger MJ. Langmuir 2000;16:8952.
[67] Oberdisse J. Phy Chem Chem Phys 2004;6(7):1557–61.
[68] Zajac J, Chorro C, Lindheimer M, Partyka S. Langmuir 1997;13 (6):1486–95.
[69] Alami E-O, Holmberg K. Adv Colloid Interface Sci 2003;100–102: 13–46.
[70] Langmuir I. J Am Chem Soc 1918;40:1361.
[71] Huang L, Shrotri S, Somasundaran P. JCIS 1997;92(1):179–83.
[72] Cases JM, Poirier JE, Canet D. In: Cases JM, editor. Solid–liquid interactions in porous media. Paris: Technip Publisher; 1985.
[73] Łjajtat L, Narkiewicz-Michałek J, Rudzinski W, Partyka S. Langmuir 1993;9:3174.
[74] Drach M, Andrzejewska A, Narkiewicz-Michałek J. Appl Surf Sci 2005;252(3):730–44.
[75] Johnson RA, Nagarajan R. Colloids Surf, A Physicochem Eng Asp 2000;167(1–2):21–30.
[76] Levitz P. Langmuir 1991;7:1595.
[77] Scheutjens JMHM, Fleer GJJ. J Phys Chem 1979;83:1619.
[78] Leermakers FAM, Scheutjens JMHM. J Phys Chem 1988;89:3264.
[79] Bohmer MR, Koopal LK. Langmuir 1992;8:1594.
[80] Reimer U, Wahab M, Schiller P, Mogel H-J. Langmuir 2001;17:8444.
[81] Gu T, Zhu B. Colloids Surf 1990;44:81.
[82] Zhu B, Gu T. Adv Colloid Interface Sci 1991;37:1–32.
[83] Kunjappu JT, Somasundaran P. Colloids Surf 1989;38(4):305–11.
[84] Kunjappu JT, Somasundaran P. Colloids Surf, A 1989;37:245.
[85] Manne S, Gaub HE. Science 1995;270:1480–2.
[86] Warr GG. Curr Opin Colloid Interface Sci 2000;5(1,2):88–94.
[87] Ducker WA. In: Mittal KL, Shah DO, editors. Adsorption and aggregation of surfactants in solution, vol. 109. New York: Marcel Dekker; 2003. p. 219–42.
[88] Schulz JC, Warr GG, Hamilton WA, Butler PD. J Phys Chem, B 1999;103(50):11057–63.
[89] Wong K, Cabane B, Somasundaran P. Colloids Surf, A 1988;30: 355–60.
[90] Fu E. DES thesis, Columbia University, 1987.
[91] Somasundaran P, Fu E, Xu Q. Langmuir 1992;8:1065.
[92] Xu Q. Doctoral thesis. Mechanisms of ionic–nonionic surfactant mixture adsorption at solid/liquid interfaces – a study of adsorption, fluorescence spectroscopy and mathematical modeling. Columbia University, 1992.
[93] Huang Z, Yan Z, Gu T. Colloids Surf 1989;36:353.
[94] Thibaut A, Misselyn-Bauduin AM, Grandjean J, Broze G, Jerome R. Langmuir 2000;16:9192–8.

[95] Brinck J, Tiberg F. Langmuir 1996;12(21):5042–7.
[96] Porter-Koltalo F, Desbene PL, Treiner C. Langmuir 2001;17:3858–62. Portet F, Desbene PL, Treiner C. J Colloid Interface Sci 2001;194:379–91.
[97] Zhang L, Somasundaran P. JCIS 2006;302(1):20–4.
[98] Xu Q, Vasudevan TV, Somasundaran P. JCIS 1991;142:528.
[99] Huang L, Maltesh C, Somasundaran P. JCIS 1996;177:222.
[100] Huang L, Shrotri S, Somasundaran P. JCIS 1997;192:179.
[101] Huang L, Somasundaran P. Langmuir 1996;12(24):5790–5.
[102] Huang L, Somasundaran P. Langmuir 1997;13(25):6683–8.
[103] Zhang L, Zhang R, Somasundaran P. JCIS 2006;302(1):20–4.
[104] Lokar WJ, Ducker WA. Langmuir 2004;20:4553–8.
[105] Portet F, Desbene PL, Treiner C. JCIS 1996;184(1):216–26.
[106] Zhang R. Doctoral of Engineering Science Thesis, Columbia University, 2005.
[107] Zhang R, Somasundaran P. Langmuir 2004;20:8552–8.
[108] Zhang R, Somasundaran P. Langmuir 2005;21(11):4868–73.
[109] Israelachvilli JN, Mitchell DJ, Ninham BW. J Chem Soc, Faraday Trans, II Molec Chem Phys 1976;72(9):1525–68.
[110] Kapur PC, Healy TW. Colloids Surf 2002;205:101.